Novel Antitransferrin Receptor Antibodies Improve the Blood-Brain Barrier Crossing Efficacy of Immunoliposomes

(Article begins on next page)

24 November 2024

Novel Antitransferrin Receptor Antibodies Improve the Blood-Brain Barrier Crossing Efficacy of Immunoliposomes

Maria Gregori, Antonina Orlando, Silvia Sesana, Luca Nardo, Domenico Salerno, Francesco Mantegazza, Francesca Re, Fabio Malavasi, Massimo Masserini, Emanuela Cazzaniga.

Abstract

Surface functionalization with antitransferrin receptor (TfR) mAbs has been suggested as the strategy to enhance the transfer of nanoparticles (NPs) across the blood-brain barrier (BBB) and to carry nonpermeant drugs from the blood into the brain. However, the efficiency of BBB crossing is currently too poor to be used in vivo. In the present investigation, we compared 6 different murine mAbs specific for different epitopes of the human TfR to identify the best performing one for the functionalization of NPs. For this purpose, we compared the ability of mAbs to cross an in vitro BBB model made of human brain capillary endothelial cells (hCMEC/D3). Liposomes functionalized with the best performing mAb (MYBE/4C1) were uptaken, crossed the BBB in vitro, and facilitated the BBB in vitro passage of doxorubicin, an anticancer drug, 3.9 folds more than liposomes functionalized with a nonspecific IgG, as assessed by confocal microscopy, radiochemical techniques, and fluorescence, and did not modify the cell monolayer structural or functional properties. These results show that MYBE/4C1 antihuman TfR mAb is a powerful resource for the enhancement of BBB crossing of NPs and is therefore potentially useful in the treatment of neurologic diseases and disorders including brain carcinomas.

Introduction

In spite of decades of research, the specific transport of drugs and imaging agents to the brain remains challenging because of the efficiency of the blood–brain barrier (BBB), a tightly packed layer of endothelial cells that protect the brain from potentially harmful endogenous compounds and xenobiotics.[1] Several strategies bypassing the BBB have been proposed,[2, 3] but the potential benefits of such systems must be weighted against their impact on the defensive function of BBB. In this context, targeted delivery achieved by directly coupling a brain-targeting ligand to a drug molecule or by encapsulating drugs into brain-targeted nanoparticles (NPs) has been proposed as an innovative and noninvasive tool for delivering drugs to the brain. NP-mediated brain drug delivery might be achieved by functionalizing the NP surface with BBB targeting agents, thus allowing the NP to cross the BBB by exploiting the physiological mechanisms of transport.[4] Transferrin receptor (TfR), also known as CD71, has received the greatest attention for use in target-mediating NP brain entry, owing to its expression on BBB endothelial cells for the regulation of brain uptake of iron.[5, 6]

The purpose of this investigation was to identify, among a panel of antihuman TfR mAbs, the most efficient to promote BBB crossing of nanoliposomes (nano-LIPs)—colloidal vesicles formed by biodegradable and biocompatible phospholipids and sphingolipids frequently used as a delivery system for drugs. For this reason, 6 antihuman TfR mAbs, specific for different epitopes of the human TfR I, namely CB26 (IgG1), CBMIEL-2 (IgG1), MYBE/4G3 (IgG1), MYBE/5F5 (IgG1), MYBE/4C1 (IgG1), and CBMIEL-1 (IgM) were prepared. The criteria for selection were the mAb ability to cross an *in vitro* BBB model made up of human brain capillary endothelial cells (hCMEC/D3). The best performing mAb was used to functionalize LIP, and the permeability across the BBB model of the resulting functionalized NP was studied to verify their potential as nanocarriers for applications in the treatment of brain diseases.

Experimental

Materials

Bovine brain sphingomyelin (Sm), cholesterol (Chol), and 1,2-distearoyl-sn-glycero-3-phospho-ethanolamine-N-[maleimide(polyethyleneglycol)-2000] were purchased from Avanti Polar Lipids, Inc. (Alabaster, AL). *N*-(4,4-difluoro-5,7-dimethyl-4-bora-3a,4a-diaza-s-indacene-3-dodecanoyl)-sphingosyl-phosphocholine (BODIPY-Sm) was from Molecular Probes (Life Technologies, Carlsbad, CA). *N*-acetyl-cysteine, Sepharose CL-4B, doxorubicin hydrochloride(DOX), 3-(4,5-

dimetiltiazol-2-yl)-2,5-diphenyltetrazolium bromide (MTT),4-(2-hydroxyethyl) piperazine-1-ethanesulfonic acid (HEPES), and Triton X-100 were purchased from Sigma-Aldrich. Tritiated sphingomyelin ($[^3H]$-Sm) was from PerkinElmer (Waltham, MA). Amicon Ultra-15 centrifugal 10K filter devices and polycarbonate filters for the extrusion procedure were purchased from Merck Millipore (Billerica, MA). The Thermobarrel Extruder was from LipexBiomembranes (Vancouver, BC, Canada). Purified rat antimouse RI7217 was from BioLegend (San Diego, CA). Ultrapure and deionized water were obtained from Direct-Q5n system (Millipore, Italy). All other chemicals were reagentgrade. All the stock solutions for cell cultures were from Euroclone (Milano, Italy). The Elisa kits for IgM and IgG quantitative detection were from eBioscience (San Diego, CA). Texas Red-X phalloidin and 4′,6-diamidino-2-phenylindole were from Molecular Probes (Life Technologies, Carlsbad, CA).

Methods

Preparation of Antihuman TfR mAbs

A panel of specific murine mAbs was produced through immunization with murine L-fibroblasts transfected with the human TfR-1 (L-CD71^{+}), obtained as described.[7] Female Balb/c mice were injected twice intraperitoneally with 5×10^6 cells. Five days before somatic fusion with the P3.X63.Ag8/653 myelomaline, mice were injected intravenously with 2×10^6 cells. Four days after the last injection, the spleen was removed for fusion using conventional techniques.[8] The reactivity of the individual anti-CD71 mAbs was analyzed by cytofluorimetric analysis (see later). Positive clones underwent 2 rounds of cultures after limiting dilution and were then expanded in massive cultures. Individual clones were tested for isotype by means of Outcherlony technique. The mAbs identified were CB26 (IgG1), CB-MIEL-2 (IgG1), MYBE/4G3 (IgG1), MYBE/5F5 (IgG1), CB-MIEL-1 (IgM), and MYBE/4C1 (IgG1). Each mAb was purified using an HPLC technique as described.[9] The purified mAbs were then sterilized by 0.22-μm filtration (Millipore Polyethersulfone Millex-GP Syringe Filter Unit, radiosterilized) and detoxified by Detoxi-Gel Endotoxin Removing Gel (Thermo Scientific). The work for the production of the murine mAbs was performed under the control of a local Committee of Animal Care, after a permission issued by the Istituto Superiore di Sanità (National Institute of Health, Rome).

Cytofluorimetric Analysis

L-CD71^{+} cells (2.5×10^5) washed in phosphate-buffered saline (PBS) containing 1% bovine serum albumin and NaN_3 were incubated with the panel of anti-CD71 mAbs (1 h, 4°C). Unbound mAb

was eliminated by washing twice and incubated 30 min, 4°C with fluorescein isothiocyanate (FITC)-conjugated F(ab')2 goat antimouse IgG+IgM (Jackson Immuno-Research Laboratories, West Grove, PA). The samples were washed, resuspended in PBS, and acquired on an FACScan (Becton-Dickinson, San Jose, CA) using CellQuest Software (Becton-Dickinson). Data WinMDI 2.9 software collected were analyzed using a WinMDI 2.9 software (Scripps Research Institute, La Jolla, CA). IB4 was analyzed with a similar approach using murine NIH-3T3 cells trasfected with human CD38 (NIH-3T3/CD38+). Mock-transfected L-cells were used as negative controls.

Preparation of LIP Functionalized With mAbs (MYBE/4C1-LIP, IB4-LIP, and RI7217-LIP)

LIPs were prepared in 10 mM PBS, pH 7.4, using Sm/Chol/1,2-distearoyl-sn-glycero-3-phospho-ethanolamine-N-[maleimide(polyethyleneglycol)-2000 (49.5:49.5:1 molar ratio), by extrusion of the multilamellar vesicles through 100-nm pore-size filters, as previously described.[10] For preparation of fluorescently labeled LIP, 0.5 molar% of total Sm was substituted with BODIPY-Sm. For preparing radiolabeled LIP, 0.001 molar% of [3H]-Sm (100 μCi/mL) was added as a tracer to track lipid distribution by measuring radioactivity. For the covalent coupling to maleimide-containing LIP, MYBE/4C1, IB4, and RI7217 were thiolated, as described.[10] Thiolated mAbs were then incubated with LIP (4 mM) overnight at 25°C at a 1:1000 molar ratio of mAbs/phospholipids. Unbound mAbs were removed by using gel exclusion chromatography (Sepharose 4B-CL column). The amount of mAb bound to LIP was quantified using the Bradford assay.[11] Phospholipids in final samples were quantified by using Stewart's assay.[12] mAb-functionalized LIPs are called IB4-LIP, MYBE/4C1-LIP, and RI7217-LIP.

Preparation of DOX-Loaded LIP (MYBE/4C1-DOX-LIP, IB4-DOX-LIP, and RI7217-DOX-LIP)

The procedure described by Sakakibara et al.[13] was followed with only small changes. LIPs composed as previously described were prepared in ammonium sulfate (500 mM, pH 5.5) and extruded through polycarbonate membranes of 100-nm pores. LIPs were then dialyzed against HEPES (10 mM, pH 7.4) and incubated with DOX for 1 h at 65°C. Free DOX was removed by gel filtration (Sepharose 4B-CL column). DOX loading was quantified fluorometrically ($\lambda_{ex} =$ 495 nm; $\lambda_{em} =$ 592 nm) after vesicle disruption with 0.1% Triton X-100.[14] To obtain DOX concentration in the solution, fluorescence intensities were compared with a previously established calibration curve for DOX in HEPES (10 mM, pH 7.4). Drug loading was calculated using the following equation: drug loading% = DOX concentration in NP solution or NP concentration in the same solution × 100. LIPs were then functionalized with mAbs as described previously.

Size and Charge Characterization of LIP

Size, ζ-potential, polydispersity index, and stability were analyzed by dynamic light scattering (DLS), as described previously.[15] The reported data are the mean of at least 5 different measurements.

Cell Cultures

Immortalized hCMEC/D3 were provided by the Institut National de la Santé et de la Recherche Médicale, Paris, France) and cultured as previously described.[16]

Cellular Uptake of mAb-Functionalized LIP by Human Brain Endothelial Cells

hCMEC/D3 (65,000 cells cm^{-2}) were cultured for 2 days on rat type I collagen-coated cover slips (diameter, 22 mm) positioned in culture dishes and then incubated with fluorescent (BODIPY-Sm) IB4-LIP or MYBE/4C1-LIP (30 μg mL^{-1}of mAbs) at 37°C. After 2 h, cells were treated as described.[10] Cellular uptake of LIP was assessed by using an inverted confocal microscope (Carl Zeiss Meditec AG, Jena, Germany, model Cell Observer), equipped with a Plan-Neofluar 63x /1.4 numerical aperture oil immersion objective (Zeiss) and interfaced with a spinning-disk module (Yokogawa CSU X1) and with an EMCCD camera (Evolve 512; Photometrics, Tucson, AZ).

Evaluation of Anti-TfR mAbs or LIP or DOX Crossing of Human Brain Endothelial Cells BBB Model

hCMEC/D3 cells (passages 25-35) were seeded on 12-well transwell inserts coated with type I collagen at a density of 7×10^4 cells/cm^2 and cultured as described previously. Cells were treated when the transendothelial electrical resistance (TEER) value (measured by EVOMX meter, STX2 electrode; World Precision Instruments, Sarasota, FL) was highest. The functionality of cell monolayers was assessed by measuring the endothelial permeability (EP) of [^{14}C]-sucrose and [^{3}H]-propranolol as described.[17] Cells were incubated with different mAbs or radiolabeled LIP functionalized with mAbs or LIP functionalized with mAbs and loaded with DOX or free DOX (300 nmols/well of lipids, 15 μg/well of mAb, and 2.5 μg/well of DOX). After 2 h, the amount of anti-TfR mAbs or LIP or DOX in the 2 chambers was measured by different techniques. The amount of anti-TfR mAbs was measured using a specific ELISA kit according to the manufacturer's instructions, by using for each mAb a specific calibration curve constructed with different quantities (from 100 to 1.5 ng mL^{-1}) of the mAb analyzed. The amount of LIP was measured by radioactivity counting. The amount of DOX was measured by fluorescence, after vesicle disruption as reported previously.[14] After this, the EP across the cell monolayers was calculated as described.[17] For DOX,

results are expressed also as the percentages of the total applied dose of DOX quantified in the lower chamber.

Assessment of LIP Biocompatibility

hCMEC/D3 cells were treated with different LIP samples (MYBE/4C1-LIP, IB4-LIP, MYBE/4C1-DOX-LIP, and IB4-DOX-LIP) or with free DOX at DOX concentration of 6, 12.5, and 25 µg mL^{-1} for 2 h or 72 h, and the LIP biocompatibility was evaluated by MTT assay[18] and lactate dehydrogenase(LDH) test[19] to evaluate the mitochondrial activity and the release of the cytoplasmic enzyme LDH as a consequence of membranes leaking of damaged or dead cells, respectively. MTT solution was added to the cells for a final concentration of 0.5 mg mL^{-1}, and the cells were incubated at 37°C for 2 h. After incubation, ethanol was added to each well to dissolve the formazancrystals formed. Absorbance at 550 nm was measured with a microplate reader (Victor3 1420 multilabel counter; PerkinElmer). Untreated cells were used as a negative control. Each sample was analyzed at least 3 times. LDH was analyzed using the cytotoxicity detection kit according to the manufacturer's instruction (Roche, Germany). Absorbance at 490 nm was measured with a microplate reader (Victor3 1420 multilabel counter; PerkinElmer). The relative amount of released LDH was normalized to the total amount of LDH of control cells completely. Each sample was analyzed at least in triplicate. Moreover, TEER was also determined on hCMEC/D3 cells seeded on transwell inserts after 2 h of treatment with different LIP to assess the effect of LIP on monolayer integrity.

Statistical Analysis

All experiments were carried out at least 3 times. Statistical analyses were performed using OriginPro8 (OriginLab Corporation, Northampton, MA). Data were compared using the unpaired Student t-test and expressed as means ± SEM.

Results

Evaluation of the Reactivity of anti-TfR mAbs

The reactivity and specificity of 6 different anti-TfR mAbs were tested in indirect immune fluorescence by using as targets murine L-fibroblasts transfected with human CD71 (L-CD71^{+}). Cytofluorimetric analysis indicated that the binding of the purified mAbs was specific, and the

reactivity was maintained up until the concentration of 10 μg/mL. Only exception was for the CBMIEL-2 mAb (Fig. 1).
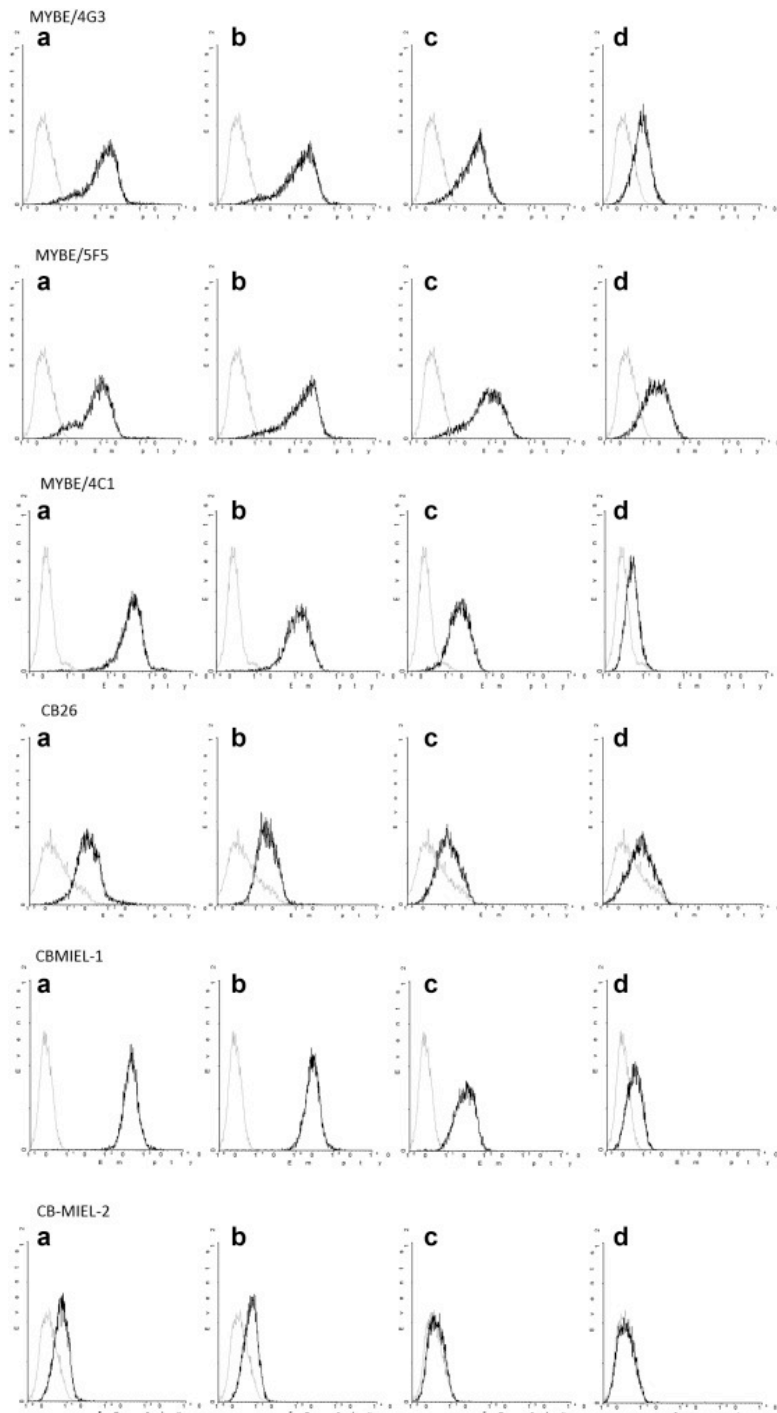

Figure 1. Comparative analysis of the different anti-CD71 mAbs under analysis. The reactivity and specificity of the individual mAbs are assessed by using murine fibroblasts transfected with human CD71 (L-CD71$^+$). Tests were done on a FACScan™ (Becton Dickinson) using an FITC-labeled F(ab')2 antimurine IgG antibody. Black profiles indicate the expression levels of the mAbs under analysis. Gray profiles are referred to an irrelevant control Ig (background). The mAbs were equalized for concentration (a: 1 mg/mL; b: 0.1 mg/mL; c: 0.01 mg/mL; and d: 0.001 mg/mL). X-axis: fluorescence intensity/cells and y-axis: number of cells registered/channel.

Evaluation of Anti-TfR mAbs Crossing of a BBB Model

Six murine mAbs specific for different epitopes of the human TfR I have been evaluated for their ability to cross an *in vitro* BBB model made up of human brain capillary endothelial cells (hCMEC/D3). Of the panel of specific TfR mAbs prepared, the MYBE/4C1 mAb provided the best results in terms of BBB crossing (Fig. 2).
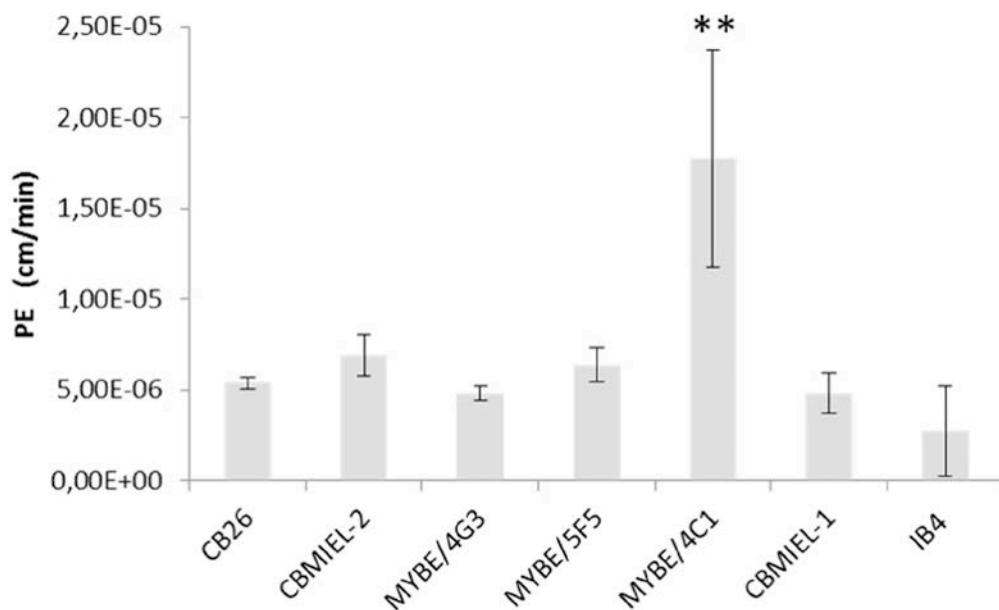

Figure 2. Transcytosis of anti-TfR mAbs. 7×10^4 hCMEC/D3 cells were incubated with 6 anti-TfR mAbs (CB26, CB-MIEL-2, MYBE/4G3, MYBE/5F5, CB-MIEL-1, and MYBE/4C1) and with a nonspecific IgG (IB4) for 3 h at 37°C, 5% CO_2. The permeability of mAbs across the cell monolayer was analyzed by specific Elisa kit. Each value is the mean of at least 3 independent experiments, and the SDs of means are presented as bars. **$p < 0.01$.

Preparation and Characterization of LIP

LIPs were functionalized with MYBE/4C1 mAb, the best performing anti-TfR mAb in terms of BBB model crossing, and, for comparison, with IB4, a nonspecific IgG, and with RI7217, an antimouse TfR mAb commercially available. To be linked to LIP surface by covalent coupling, mAbs were thiolated by Traut reaction. SDS–PAGE experiments were run to analyze the quality of MYBE/4C1 mAb after thiolation. Results showed that thiolation did not affect the integrity of the mAb (Fig. S-2). Moreover, a dot blot experiment with human TfR was performed with MYBE/4C1 mAb before and after thiolation to verify if the reaction affects the affinity of the mAb to its target. Results showed that the thiolated MYBE/4C1 mAb retained the ability of native antibody to bind human TfR (Fig. S-3). The structure of immunoLIP is depicted in Figure 3. LIPs were functionalized with mAb by covalent coupling of the thiolated mAb on the maleimide moiety

protruding from the LIP surface. This reaction allowed the linkage of 40-45 mAb molecules on the surface of each LIP, as assessed by Bradford assay. The number of mAbs conjugated per LIP was based on the assumption that a 100-nm–size liposome contains ~100,000 molecules of phospholipids.[20] To verify the presence of the antihuman TfR mAb on LIP surface, a dot blot with human TfR was run. Results showed that the MYBE/4C1 mAb is present on LIP and still binds human TfR (Fig. S-3).
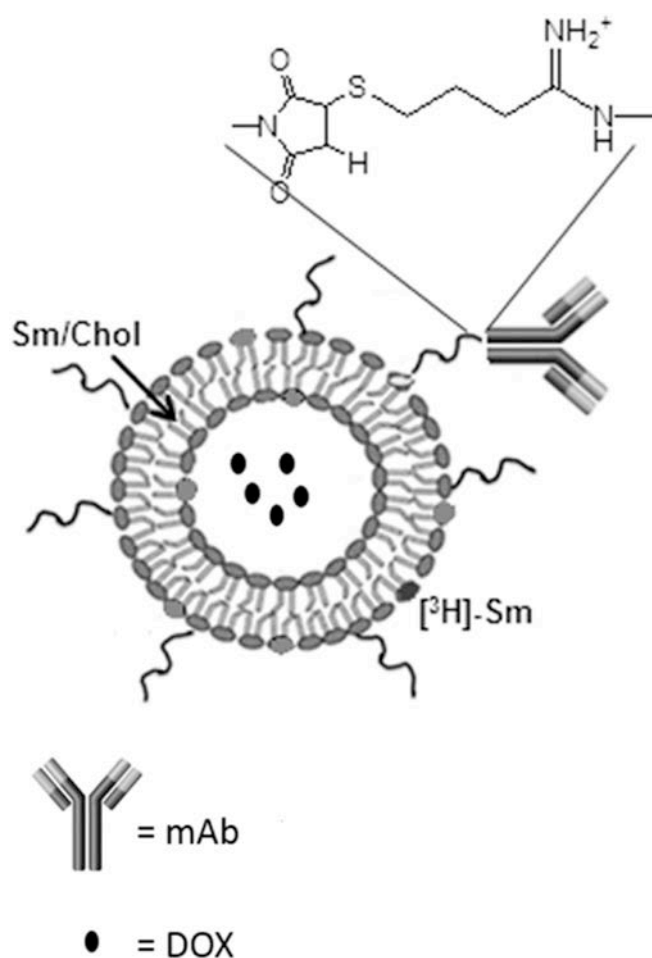

Figure 3. Hypothetical structure of LIPs double functionalized with mAbs and with DOX. DOX was incorporated into the LIPs after extrusion by a transmembrane pH gradient. mAbs were linked to LIPs by covalent coupling after thiolation (see Methods section for details).

To investigate the ability of these nanosystems to deliver drugs, DOX was used as a model drug to be incorporated into LIP before its functionalization with mAbs. Incorporation efficiency was 230 µg of DOX/mg of lipids. The size and charge of different LIPs prepared in the present investigation are reported in Table 1. All LIP preparations resulted monodispersed (polydispersity index < 0.1)

and negatively charged. Functionalization with mAbs and loading with DOX caused a slight increase of the LIP size, as already reported. All the preparations remained stable in size and charge for up to 7 days (Table 1) as accessed by DLS measurements.

Table 1. Size and Charge of LIPs

Sample	Size (nm) ± SD	Size (nm) ± SD at day 7	Z-Pot (mV) ± SD	Z-Pot (mV) ± SD at day 7
LIP	104 ± 4	106 ± 6	−25.5 ± 0.8	−23.4 ± 2.2
MYBE/4C1-LIP	125 ± 5	124 ± 3	−23.4 ± 1.2	−22.8 ± 1.0
IB4-LIP	123 ± 6	126 ± 3	−21.1 ± 2.3	−22.3 ± 1.5
RI7217-LIP	121 ± 2	119 ± 5	−27.1 ± 3.2	−27.3 ± 2.5
MYBE/4C1-DOX-LIP	142 ± 4	146 ± 5	−18.2 ± 4.0	−18.4 ± 3.1
IB4-DOX-LIP	138 ± 3	142 ± 4	−15.2 ± 3.8	−15.6 ± 2.2
RI7217-DOX-LIP	133 ± 6	133 ± 5	−24.3 ± 2.5	−23.9 ± 2.0

Mean diameter and Zeta-potential (Z-pot) were obtained by DLS and Zeta-potential analyzer for different LIPs before and after functionalization with mAbs and DOX, at day 0 and 7 after preparation.

Cellular Uptake of mAbs-Functionalized LIP by Human Brain Endothelial Cells

To investigate the cellular uptake of mAbs-functionalized LIP on the *in vitro* BBB model, BODIPY-Sm, a fluorescent phospholipid, was incorporated into LIP before functionalization with mAbs. Cellular uptake of fluorescent IB4-LIP and MYBE/4C1-LIP was investigated qualitatively by confocal microscopy on hCMEC/D3 cells. Confocal microscopy images reveal that the uptake of LIP was higher after functionalization with MYBE/4C1. Furthermore, these NPs did not induce changes in actin organization of hCMEC/D3 cells (Fig. 4).
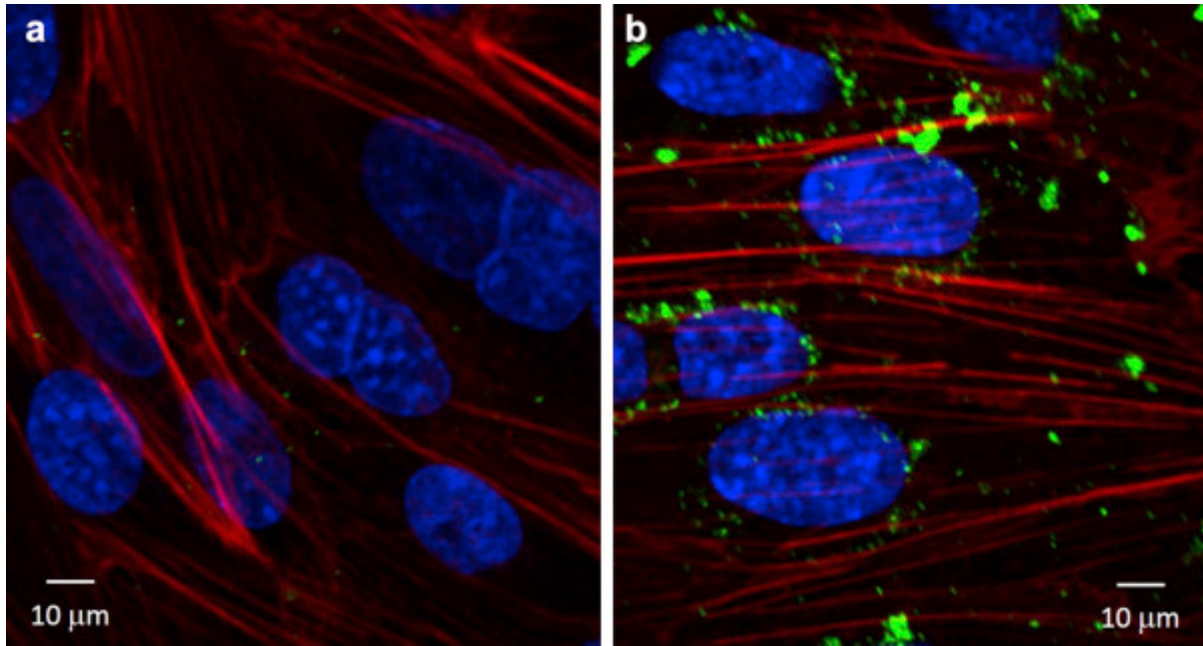
Figure 4. Confocal spinning disk microscopy of hCMEC/D3 cells after incubation with fluorescent IB4-LIP (a) (anti-human CD38, an irrelevant IgG control) or MYBE/4C1-LIP (b) (30 μg mL^{-1} of antibodies) at 37°C, 5% CO_2 saturation. Cells were incubated with phalloidin to visualize the actin filaments (red fluorescence); nuclear staining was highlighted by 4′,6-diamidino-2-phenylindole (blue fluorescence).

Permeability of mAbs-Functionalized LIP and DOX Across Human Brain Endothelial BBB Cellular Model

The permeability of MYBE/4C1-LIP across a BBB *in vitro* model made of hCMEC/D3 cells was quantitatively evaluated using [^{3}H]-Sm-labeling and radioactivity counting and compared with the permeability of free DOX and of LIP functionalized with a nonspecific mAb (IB4-LIP) and with another antimouse TfR mAb, commercially available (RI7217-LIP). hCMEC/D3 cells, grown on transwell membrane inserts, were incubated with different LIP preparations on day 12, when the maximal TEER value was registered (63 ± 5 Ω · cm^2). Transport of [^{14}C]-sucrose and [^{3}H]-propranolol was measured to access the formation of junctions with EP values of 1.48×10^{-3} cm/min and 3.51×10^{-3} cm/min, respectively, in agreement with the values reported in the literature.[21] NPs were added in the upper compartment, and the radioactivity was measured in the lower compartment after 2-h incubation. The EP across the cell monolayers was higher for MYBE/4C1-LIP ($3.69 \pm 0.078 \times 10^{-5}$ cm/min), as compared with IB4-LIP ($7.69 \pm 0.021 \times 10^{-6}$ cm/min) ($p < 0.01$) and also to RI7217-LIP ($3.31 \pm 0.07 \times 10^{-5}$ cm/min) ($p < 0.01$) (Fig. 5).
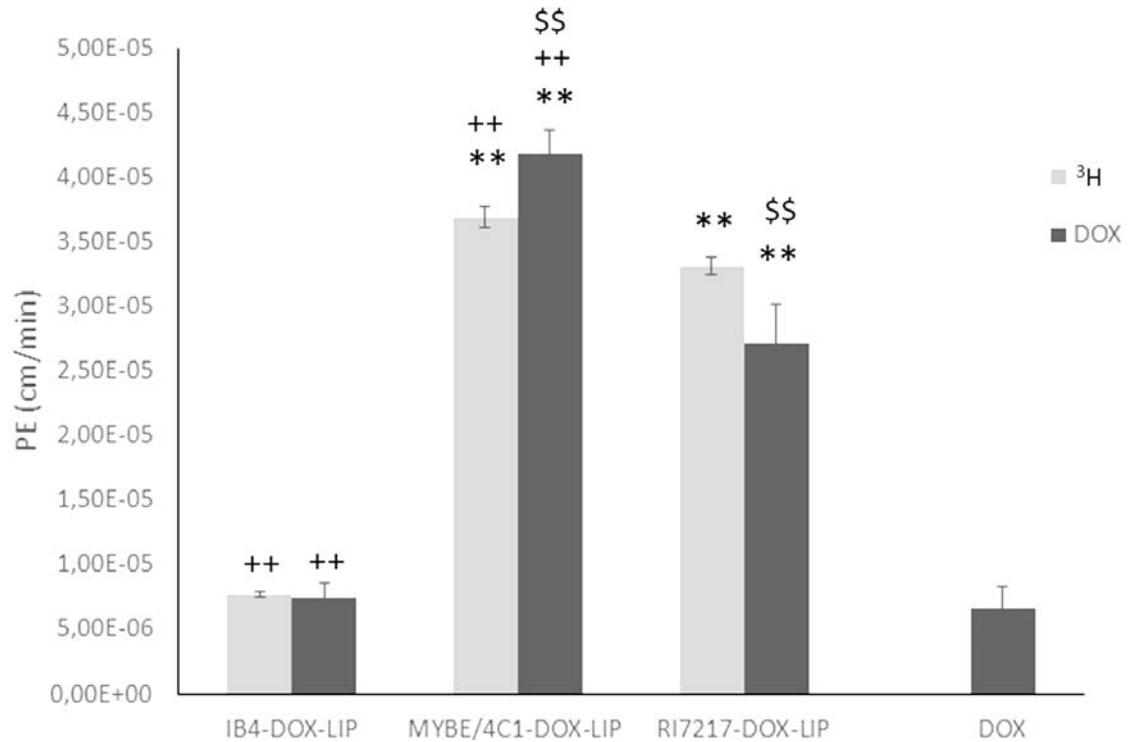
Figure 5. Cellular permeability of LIP and free DOX through hCMEC/D3 cell monolayers. $7 - 10^4$ cells were incubated with free DOX or with LIP functionalized with mAbs (IB4, MYBE/4C1, or RI7217) and with DOX and radiolabeled with $[^3H]$-Sm for 3 h at 37°C, 5% CO_2. The permeability of LIP across the cell monolayer was calculated for $[^3H]$-Sm (gray bars) and for DOX (black bars). Each value is the mean of at least 3 independent experiments, and the SDs of means are presented as bars. **$p < 0.01$ versus IB4-LIP, [++]$p < 0.01$ versus RI7217-DOX-LIP, [$$]$p < 0.01$ versus free DOX (Student t-test).

DOX PE was also investigated through the same *in vitro* BBB model by using mAbs-functionalized LIP loaded with DOX. Again, LIPs were added on the apical side of a transwell system made of hCMEC/D3 cells, and DOX in the lower compartment was quantified. The amount of DOX in the lower compartment was 0.95% ± 0.06% for MYBE/4C1-DOX-LIP, 0.24% ± 0.04% for IB4-DOX-LIP, and 0.86% ± 0.08% for RI7217-DOX-LIP. Also the EP of DOX is higher with MYBE/4C1-DOX-LIP (4.18 ± 0.14 × 10^{-5} cm/min), as compared with IB4-DOX-LIP (7.38 ± 0.12 × 10^{-6} cm/min) ($p < 0.01$), to RI7217-LIP (2.71 ± 0.30 × 10^{-5} cm/min) ($p < 0.01$) and to free DOX (6.65 ± 1.60 × 10^{-6} cm/min) (Fig. 5). To understand if the enhanced BBB *in vitro* passage of MYBE/4C1-LIP compared with RI7217-LIP is because of a higher affinity of the first mAb to human TfR, the binding of the 2 mAbs toward human TfR was investigated by surface plasmon resonance. The calculated K_D was 64.3 and 14.5 nM for MYBE/4C1 and RI7217, respectively (Fig. S-1).

Cytotoxicity

hCMEC/D3 cells were treated with different mAbs-functionalized LIP loaded or not with DOX (25 μg mL^{-1}) for 2 h, and cell viability was assessed by MTT assay and LDH test. Treatment did not affect the viability of endothelial cells (Fig. S-4). Moreover, after hCMEC/D3 incubation with LIP, the TEER value did not change within the experimental error (<3%). The effect of DOX released by LIP was observed after 72 h at different DOX concentrations. As shown in Figure 6, it was dose dependent. The calculated IC$_{50}$ of MYBE/4C1-DOX-LIP, IB4-DOX-LIP, and free DOX was 38.4 ± 4.0, 39.0 ± 4.0, and 8.7 ± 0.7 μg mL^{-1}, respectively.
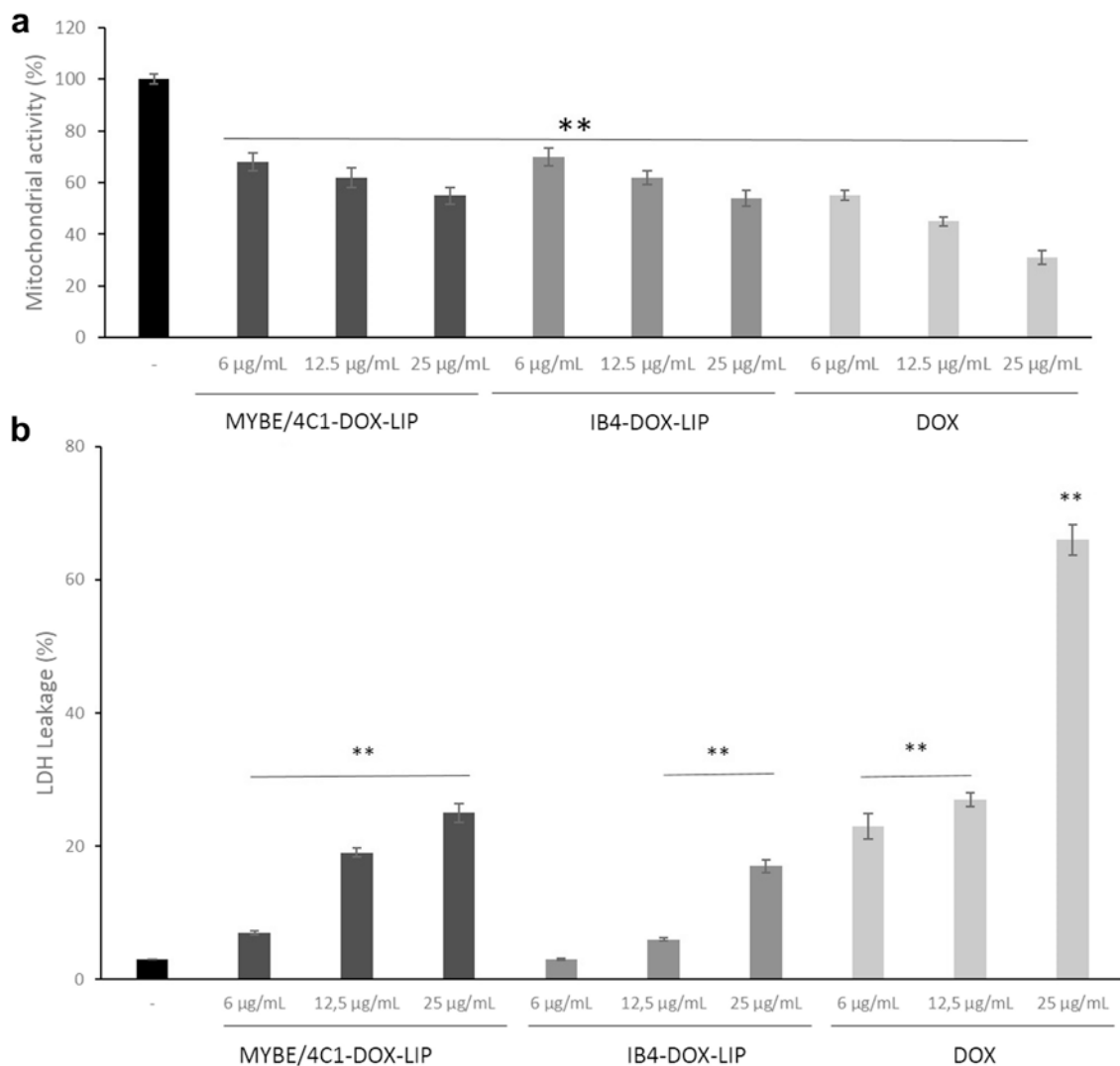

Figure 6. Cytotoxicity of mAbs and DOX-functionalized LIP or free DOX on hCMEC/D3. Cells were incubated with MYBE/4C1-DOX-LIP or IB4-DOX-LIP or free DOX (6, 12.5, and 25 μg mL^{-1} of DOX concentration) for 72 h, and the mitochondrial activity and LDHleakage were determined by MTT assay (a) and LDH assay (b), respectively. The results are reported as percentage respect to the untreated cells (control). The data are reported as the mean $\pm$ SEM of triplicate experiments. The results were compared by Student t-test. - =untreated cells.

Discussion

The entry of several potentially therapeutic agents into the brain is restricted by the presence of the BBB. The use of receptor-mediated transcytosis is one of the strategies proposed to carry therapeutic agents from the blood into the brain.[22] In particular, the functionalization of NP with mAbs recognized by receptors overexpressed on BBB endothelial cells has been reported to enhance BBB passage both of NP and NP-embedded drugs.[23] Among all the receptors analyzed, TfR is the most widely studied for BBB targeting.[24]Recently, our group designed multifunctional LIP for Alzheimer disease therapy that are able to cross the BBB, thanks to the functionalization with RI7217, an antimouse TfR mAb.[10] The literature contains multiple examples of NP functionalized with antimouse or antirat TfR mAbs for crossing the BBB[25, 26, 27, 28, 29, 30]; however, very few examples concern the functionalization of NP with antihuman TfR mAbs,[31, 32, 33] and to the best of our knowledge, none of them is designed to facilitate crossing of the BBB by NP. Even if the homology between mouse and human receptor is 86%,[34] the use of antihuman TfR mAb-functionalized NP as brain drug delivery carriers is highly regarded. For this reason, we produced a panel of 6 antihuman TfR mAbs in our study and tested their ability to cross an *in vitro* BBB cellular model made up of the human brain capillary endothelial cell line hCMEC/D3, known as expressing TfR.[21] The best performing mAb, MYBE/4C1, was used to functionalize LIP to prepare brain delivery carriers. LIPs were selected as delivery vehicles because they are the most common NP currently used for targeted drug delivery *in vivo*.[35, 36] They are nontoxic, nonimmunogenic, biocompatible, biodegradable, and can be grafted with PEG on their surface to avoid rapid clearance by the reticuloendothelial system. Moreover, these carriers can store drugs or imaging agents in the hydrophobic shell or in the aqueous interior, depending on the nature of the drug or of the contrast agent being carried. The lipidic matrix used in the present investigation (Chol and Sm) was chosen because already used for *in vivo* experiments, displaying high circulation times in blood, biocompatibility, and resistance to hydrolysis.[37] A thiol-maleimide covalent coupling was exploited for mAb functionalization. Indeed, our group proved the superior efficiency of covalent coupling as compared with biotin/streptavidin ligation to link mAb to LIP surface to overcome a BBB *in vitro* model.[10] Reaction conditions were optimized to obtain 40-45 mAb molecules exposed on the surface of each LIP, a density considered as optimal for brain targeting.[25] DLS analysis showed that LIPs prepared have a size below 200 nm, which in a future *in vivo* application may allow the NP to move at appreciable rates through the brain extracellular space.[38] Moreover, the negative charge of the resulting LIP is a good feature for using them as brain carriers because it is

reported that cationic NPs are more toxic than neutral and negatively charged NP toward BBB cells.[39]

The results of the present work demonstrated that the presence of MYBE/4C1 mAb on the surface enhanced the crossing of LIP on hCMEC/D3 BBB model. The transcytosis ability of these LIPs was investigated *in vitro* by measuring the permeability values of both ^{3}H-Sm used as LIP tracer and DOX embedded in LIP across a monolayer of hCMEC/D3 cells. A great improvement in the amount of DOX carried through the BBB by using MYBE/4C1-DOX-LIP instead of the free drug is clearly evident, as already showed for other LIPs carrying DOX.[40] Moreover, EP values of LIP functionalized with MYBE/4C1 are higher than the ones obtained using LIP functionalized with a commercially available rat antimouse TfR (RI7217). Surface plasmon resonance experiments suggest that these results are because of a higher affinity of MYBE/4C1 mAb to human TfR compared with RI7217. This finding is a confirmation of the choice of adopting human TfR as a target in functionalizing NP to cross the human BBB *in vitro* model. Moreover, cell viability and monolayer integrity were not altered by the treatment.

To validate the suitability of such NP as brain drug carriers, DOX was embedded in MYBE/4C1-LIP. DOX was the first drug to be delivered by LIPs to brain tumors.[41] Many studies indicated that therapy with DOX bound to NP offers a therapeutic potential for the treatment of human brain cancer.[42, 43, 44, 45] DOX displays *in vitro* an excellent antineoplastic activity against brain tumors, but its clinical use for brain cancer is in fact limited because of severe systemic side effects[46] and because it is extruded by P-glycoprotein (ABCB1) in BBB cells.[47] The incorporation of DOX in NP may limit the side effects of the free drug and facilitate the passage of the BBB. Here, DOX incorporation was obtained by exploiting a reported procedure.[13, 14, 48] To this aim, a transmembrane pH gradient was generated using a solution of ammonium saltsat acidic pH to induce protonation of DOX and precipitation in the interior aqueous medium of LIP. The adoption of this procedure yielded a very high incorporation efficiency.

Interestingly, PE values obtained when quantifying DOX transport across the BBB model are very similar to values obtained when quantifying radioactivity of radiolabeled LIP. These results support the view that LIPs cross the BBB intact in an *in vitro* model. Significant is the observation that IC_{50} value of DOX embedded in LIP was higher than that of free DOX, suggesting the possibility of using such LIP to prevent the side effects of free drug against BBB cells.

Conclusions

The present *in vitro* study shows that LIP functionalized with MYBE/4C1, an antihuman TfR mAb, could serve as nanovectors for delivering of drugs across the BBB to the brain. The enhanced BBB crossing of the incorporated anticancer drug doxorubicin suggests the potential use of these NPs for the treatment of brain tumors.

References

1. Wolburg H, Noell S, Mack A, Wolburg-Buchholz K, Fallier-Becker P. Brain endothelial cells and the glio-vascular complex. Cell Tissue Res. 2009;335(1):75-96.

2. Bellavance MA, Blanchette M, Fortin D. Recent advances in blood-brain barrier disruption as a CNS delivery strategy. AAPS J. 2008;10(1):166-177.

3. Zhao YZ, Lu CT, Li XK, Cai J. Ultrasound-mediated strategies in opening brain barriers for drug brain delivery. Expert Opin Drug Deliv. 2013;10(7):987-1001.

4. Patel MM, Goyal BR, Bhadada SV, Bhatt JS, Amin AF. Getting into the brain: approaches to enhance brain drug delivery. CNS Drugs. 2009;23(1):35-58.

5. Burkhart A, Azizi M, Thomsen MS, Thomsen LB, Moos T. Accessing targeted nanoparticles to the brain: the vascular route. Curr Med Chem. 2014;21(36): 4092-4099.

6. Chen Y, Liu L. Modern methods for delivery of drugs across the blood-brain barrier. Adv Drug Deliv Rev. 2012;64(7):640-665.

7. Peruzzi L, Melioli G, De Monte LB, et al. Microplate selection technique (MPST). A new method for selecting mouse transfectants expressing human gene products. J Immunol Methods. 1989;123(1):113-121.

8. Deaglio S, Capobianco A, Calì A, et al. Structural, functional, and tissue distribution analysis of human transferrin receptor-2 by murine monoclonal antibodies and a polyclonal antiserum. Blood. 2002;100(10):3782-3789.

9. Horenstein AL, Durelli I, Malavasi F. Purification of clinical-grade monoclonal antibodies by chromatographic methods. Methods Mol Biol. 2005;308:191-208.

10. Salvati E, Re F, Sesana S, et al. Liposomes functionalized to overcome the bloodbrain barrier and to target amyloid-b peptide: the chemical design affects the permeability across an in vitro model. Int J Nanomedicine. 2013;8:1749-1758.

11. Bradford MM. A rapid and sensitive method for the quantitation of microgram quantities of protein utilizing the principle of protein-dye binding. Anal Biochem. 1976;72:248-254.

12. Stewart JC. Colorimetric determination of phospholipids with ammonium ferrothiocyanate. Anal Biochem. 1980;104(1):10-14.

13. Sakakibara T, Chen FA, Kida H, et al. Doxorubicin encapsulated in sterically stabilized liposomes is superior to free drug or drug-containing conventional liposomes at suppressing growth and metastases of human lung tumor xenografts. Cancer Res. 1996;56(16):3743-3746.

14. Fritze A, Hens F, Kimpfler A, Schubert R, Peschka-Süss R. Remote loading of doxorubicin into liposomes driven by a transmembrane phosphate gradient. Biochim Biophys Acta. 2006;1758(10):1633-1640.

15. Gobbi M, Re F, Canovi M, et al. Lipid-based nanoparticles with high binding affinity for amyloid-b 1-42 peptide. Biomaterials. 2010;31(25):6519-6529.

16. Re F, Cambianica I, Sesana S, et al. Functionalization with ApoE-derived peptides enhances the interaction with brain capillary endothelial cells of nanoliposomes binding amyloid-beta peptide. J Biotechnol. 2010;156(4):341-346.

17. Cecchelli R, Dehouck B, Descamps L, et al. In vitro model for evaluating drug transport across the blood-brain barrier.AdvDrugDeliv Rev. 1999;36(2-3):165-178.

18. Orlando A, Re F, Sesana S, et al. Effect of nanoparticles binding b-amyloid peptide on nitric oxide production by cultured endothelial cells and macrophages. Int J Nanomedicine. 2013;8:1335-1347.

19. Orlando A, Colombo M, Prosperi D, et al. Iron oxide nanoparticles surface coating and cell uptake affect biocompatibility and inflammatory responses of endothelial cells and macrophages. J Nanopart Res. 2015;17:351.

20. Hansen CB, Kao GY, Moase EH, Zalipsky S, Allen TM. Attachment of antibodies to sterically stabilized liposomes: evaluation, comparison and optimization of coupling procedures. Biochim Biophys Acta. 1995;1239(2):133-144.

21. Poller B, Gutmann H, Krahenbühl S, et al. The human brain endothelial cell line €hCMEC/D3 as a human blood-brain barrier model for drug transport studies. J Neurochem. 2008;107(5):1358-1368.

22. Wang YY, Lui PC, Li JY. Receptor-mediated therapeutic transport across the blood-brain barrier. Immunotherapy. 2009;1(6):983-993.

23. Gregori M, Masserini M, Mancini S. Nanomedicine for the treatment of Alzheimer's disease. Nanomedicine (Lond). 2015;10(7):1203-1218.

24. Jones A, Shusta E. Bloodebrain barrier transport of therapeutics via receptormediation. Pharm Res. 2007;24:1759-1771.

25. Huwyler J, Wu D, Pardridge WM. Brain drug delivery of small molecules using immunoliposomes. Proc Natl Acad Sci U S A. 1996;93(24):14164-14169.

26. Liu Z, Zhao H, Shu L, et al. Preparation and evaluation of Baicalin-loaded cationic solid lipid nanoparticles conjugated with OX26 for improved delivery across the BBB. Drug Dev Ind Pharm. 2015;41(3):353-356.

27. van Rooy I, Mastrobattista E, Storm G, Hennink WE, Schiffelers RM. Comparison of five different targeting ligands to enhance accumulation of liposomes into the brain. J Control Release. 2011;150(1):30-36.

28. Markoutsa E, Papadia K, Giannou AD, et al. Mono and dually decorated nanoliposomes for brain targeting, in vitro and in vivo studies. Pharm Res. 2014;31(5):1275-1289.

29. Bao H, Jin X, Li L, Lv F, Liu T. OX26 modified hyperbranched polyglycerolconjugated poly(lactic-co-glycolic acid) nanoparticles: synthesis, characterization and evaluation of its brain delivery ability. J Mater Sci Mater Med. 2012;23(8):1891-1901.

30. Ulbrich K, Hekmatara T, Herbert E, Kreuter J. Transferrin- and transferrinreceptor-antibody-modified nanoparticles enable drug delivery across the blood-brain barrier (BBB). Eur J Pharm Biopharm. 2009;71(2):251-256.

31. Wang J, Tian S, Petros RA, Napier ME, Desimone JM. The complex role of multivalency in nanoparticles targeting the transferrin receptor for cancer therapies. J Am Chem Soc. 2010;132(32):11306-11313.

32. Karlsson GB, Platt FM. Analysis and isolation of human transferrin receptor using the OKT-9 monoclonal antibody covalently crosslinked to magnetic beads. Anal Biochem. 1991;199(2):219-222.

33. Rubovszky B, Hajdú P, Krasznai Z, et al. Detection of channel proximity by nanoparticle-assisted delaying of toxin binding; a combined patch-clamp and flow cytometric energy transfer study. Eur Biophys J. 2005;34(2):127- 143.

34. Wang E, Obeng-Adjei N, Ying Q, et al. Mouse mammary tumor virus uses mouse but not human transferrin receptor 1 to reach a low pH compartment and infect cells. Virology. 2008;381(2):230-240.

35. Allen TM, Cullis PR. Liposomal drug delivery systems: from concept to clinical applications. Adv Drug Deliv Rev. 2013;65(1):36-48.

36. Chang HI, Yeh MK. Clinical development of liposome-based drugs: formulation, characterization, and therapeutic efficacy. Int J Nanomedicine. 2012;7: 49-60.

37. Webb MS, Harasym TO, Masin D, Bally MB, Mayer LD. Sphingomyelincholesterol liposomes significantly enhance the pharmacokinetic and therapeutic properties of vincristine in murine and human tumour models. Br J Cancer. 1995;72:896-904.

38. Nance EA, Woodworth GF, Sailor KA, et al. A dense poly(ethylene glycol) coating improves penetration of large polymeric nanoparticles within brain tissue. Sci Transl Med. 2012;4(149):149ra119.

39. Lockman PR, Koziara JM, Mumper RJ, Allen DD. Nanoparticle surface charges alter blood-brain barrier integrity and permeability. J Drug Target. 2004;12(9-10):635-641.

40. Pinzon-Daza M, Garz on R, Couraud P, et al. The association of statins plus LDL receptor-targeted liposome-encapsulated doxorubicin increases in vitro drug delivery across blood-brain barrier cells. Br J Pharmacol. 2012;167(7): 1431-1447.

41. Siegal T, Horowitz A, Gabizon A. Doxorubicin encapsulated in sterically stabilized liposomes for the treatment of a brain tumor model: biodistribution and therapeutic efficacy. J Neurosurg. 1995;83(6):1029-1037.

42. Steiniger SC, Kreuter J, Khalansky AS, et al. Chemotherapy of glioblastoma in rats using doxorubicin-loaded nanoparticles. Int J Cancer. 2004;109(5): 759-767.

43. Lin J, Shigdar S, Fang DZ, et al. Improved efficacy and reduced toxicity of doxorubicin encapsulated in sulfatide-containing nanoliposome in a glioma model. PLoS One. 2014;9(7):e103736.

44. Yang Y, Yan Z, Wei D, et al. Tumor-penetrating peptide functionalization enhances the anti-glioblastoma effect of doxorubicin liposomes. Nanotechnology. 2013;24(40):405101.

45. Wohlfart S, Khalansky AS, Gelperina S, et al. Efficient chemotherapy of rat glioblastoma using doxorubicin-loaded PLGA nanoparticles with different stabilizers. PLoS One. 2011;6(5):e19121.

46. Ohnishi T, Tamai I, Sakanaka K, et al. In vivo and in vitro evidence for ATP-dependency of P-glycoprotein-mediated efflux of doxorubicin at the blood-brain barrier. Biochem Pharmacol. 1995;49(10):1541-1544.

47. Chlebowski RT. Adriamycin (doxorubicin) cardiotoxicity: a review. West J Med. 1979;131(5):364-368.

48. Shroff K, Kokkoli E. PEGylated liposomal doxorubicin targeted to a5b1- expressing MDA-MB-231 breast cancer cells. Langmuir. 2012;28(10): 4729-4736.